J Appl Electrochem (2010) 40:989–995
DOI 10.1007/s10800-009-9926-y

ORIGINAL PAPER

Synchronization properties of coupled electrochemical bursters

Rhythmic electrodissolution/passivation of iron electrode assemblies in acidic electrolyte containing chloride ions

Antonis Karantonis · Dimitris Koutsaftis · Niki Kouloumbi

Received: 29 November 2008 / Accepted: 30 April 2009 / Published online: 26 May 2009

Abstract In the present paper the non-linear time evolution of the electrodissolution/passivation of iron in sulfuric acid–sodium chloride solution is explored. The working electrode is an assembly of two iron disk electrodes, interacting through the electrolyte, and the time evolution of the electric current has the form of spontaneous bursting oscillations. The main aim of this work is to characterize the modes of synchrony and more specifically the synchronization of electric bursts and the synchronization of electric spikes. The characterization is based on the calculation of the firing rates from the experimental time series and the extraction of the slow dynamics by low-pass filtering. The analysis is performed both for elliptic and square wave electrochemical bursting and the results are compared with neural oscillations.

Keywords Iron electrodissolution · Passivation · Bursting oscillations · Chlorides · Electrode assemblies

1 Introduction

The analogy between electrochemical and neurophysiological systems was first proposed by W. Ostwald, in the beginning of the Twentieth century. Ostawald's and Heathcote's suggestion [1] was based on the experimental observation of the process of spontaneous activation of passive iron wires under the influence of a finite external perturbation, e.g. touching momentary the passive surface by a zinc rod.

The resemblance of electrochemical activation and the neural transmission of electric excitation was pursued even further by Lillie [2–4] and Bonhoeffer [5–7]. Indeed, their experimental findings lead them to propose the activation of passive iron as a model of nerve excitation. These ideas were later elaborated by Frank [8, 9] in relation not only to excitation but also to the spontaneous rhythmic activity. Indeed, autonomous electric oscillatory activity which is so common in the neural system was proved to be typical in a large class of electrochemical systems, spanning the fields of corrosion, electrocatalysis and electrodeposition [10–12].

The electrodissolution/passivation of iron in sulfuric acid is a characteristic example of an electrochemical process with spontaneous oscillatory behaviour. While the iron working electrode is polarized anodically in the region close to the transition from electrodissolution to passivation, the electric current oscillates periodically. During these oscillations, the electrode shifts in a cyclic manner from a passive state where the electrode surface is completely covered by an insulating film, to an active state where iron electrodissolves from a free surface.

In a series of publications it was shown that assemblies consisting of several iron electrodes immersed in a common electrolytic solution resemble neurophysiological networks to some extent [13–20]. The main aspect which determines the non-linear dynamic response of such assemblies is the synchronization of the spontaneous current oscillations, i.e. the simultaneous occurrence of current spiking. Moreover, the modes of synchrony can be tuned by varying the distance d between the interacting electrodes and, more importantly, the distance l between the working and reference electrodes. Actually, it has been shown both theoretically and experimentally [21–23] that

A. Karantonis (✉) · D. Koutsaftis · N. Kouloumbi
Department of Materials Science and Engineering, School of Chemical Engineering, National Technical University of Athens, Zografou, 15780 Athens, Greece
e-mail: antkar@central.ntua.gr

the interaction between the oscillatory electrodes can be positive (excitatory) or negative (inhibitory) for large or small l, respectively.

The spontaneous electric current oscillations observed during the electrodissolution/passivation of iron in sulfuric acid are simple periodic for potential values close to the active/passive transition. But, in the presence of small amounts of chloride ions in the electrolytic solution the simple oscillations transform to oscillations consisting of spiking interrupted by regions of quiescence [24–26]. This type of non-linear dynamic behavior is designated as bursting and it is very common in the neural system. A recent systematic analysis of the electrochemical bursting induced by chloride ions showed that there are two different types of bursting oscillations, determined by the value of the applied potential V [27]. Thus, for V values close to the transition from the state to electrodissolution to the oscillatory state, electrochemical bursting was characterized as elliptic whereas for V values close to the transition from the passive state to the oscillatory state, electrochemical bursting was characterized as square wave. These two types of bursting correspond to two different non-linear dynamic scenarios [28] and their electrochemical origin is still not understood.

In the present paper we explore the potentiostatic current response of an assembly consisting of two iron electrodes. The assembly is immersed in an electrolytic solution containing chloride ions and thus the current flowing through each electrode has the form of bursting oscillations. The two iron electrodes interact through the electrolytic solution and thus are considered as a pair of coupled electrochemical oscillators. The main aim of this work is to characterize the modes of synchrony and more specifically the synchronization of electric bursts and the synchronization of electric spikes. The characterization is based on the calculation of the firing rates from the experimental time series and the extraction of the slow dynamics by low-pass filtering. The analysis is performed both for elliptic and square wave electrochemical bursting.

2 Experimental setup and materials

An electrode assembly of two iron disk electrodes was made from Fe wires (Sigma-Aldrich, 99.9% purity) of 1 mm diameter, embedded in resin. The distance d between the electrodes was varied from 3 to 8 mm. Prior to each experiment, the electrodes were polished with a series of wet 220–2400 grit silicon carbide sand-papers and cleaned with distilled water.

The electrode assembly was used as a working electrode in a standard three-electrode arrangement with respect to a silver/silver chloride reference electrode with a Haber-Luggin capillary. The tip of the capillary was located at a distance l for the working electrodes. The counter electrode was a carbon rod ($\phi = 6.25$ mm). The potential was controlled by a potentiostat (EG&G PAR 263A). The working electrodes were connected to the potentiostat through individual resistors of 1 Ω in order to measure the response of the electrodes independently. The potential drop on each resistor was measured and stored by using a Yokogawa DL 708E digital oscilloscope equipped with an 701853-HR module. The experiments were carried out in a 0.75 M H_2SO_4 (Panreac, PA), 15 mM NaCl (Merck). A detailed description of the experimental arrangement can be found in previous articles [15, 17].

All programs used for the analysis of the experimental signals were written in FORTRAN and utilized the FFTW3 library.

3 Results

A typical polarization curve of a single Fe electrode in 0.75 M H_2SO_4, 15 mM Cl^- electrolyte, with scan rate 20 mV s^{-1}, is presented in Fig. 1. During the forward scan (dashed line) the electric current increases due to the electrodissolution of iron until it reaches a value of 5.5 mA and than forms a current plateau of about 4 mA (active state) after a small current undershoot. Due to the action of chloride ions the electrode surface is not covered completely by a passive (oxide) layer, even for highly anodic values of the applied potential. During the backward scan (full line) the active state in maintained and an oscillatory region is also observed where electric current spikes are monitored. Under potentiostatic conditions these current spikes correspond to electrochemical bursting oscillations, i.e. spontaneous oscillatory activity interrupted by regions

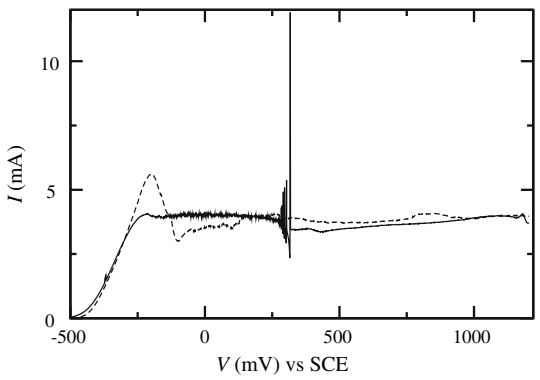

Fig. 1 Polarization curve of the Fe/0.75 M H_2SO_4, 15 mM Cl^- system with scan rate 20 mV s^{-1}. *Dashed line*: forward scan. *Full line*: Backward scan

of quiescence. As was shown in a previous publication [27], in the more cathodic neighbourhood of the oscillatory region the current response can be classified as elliptic electrochemical bursting whereas in the more anodic neighbourhood of the oscillatory region as square wave electrochemical bursting.

3.1 Synchronization of electrochemical bursts

In order to study synchronization of electrochemical bursts it is mandatory to utilize a method to separate slow burst dynamics and fast spike dynamics from the experimental time series. Unfortunately, low-pass filtering is not able to separate the dynamics, specially in the case of elliptic electrochemical bursting.

In order to extract the burst dynamics from the time series a novel methodology is introduced, based on the measurement of firing rates [29, 30]

Similarly to a previous publication [27], let us assume that the current time series $I(t)$ can be considered as a sequence of delta functions,

$$I(t) = \sum_{i=1}^{n} \delta(t - t_i), \tag{1}$$

where t_i is the spiking instance in the time series and n the total number of spikes within the duration T of a single experiment. The variation of the spiking activity $I(t)$ as a function of time can me measured by the approximate time-dependent firing rate, $r(t)$,

$$r(t) = \sum_{i=1}^{n} w(t - t_i) \tag{2}$$

where $w(t-t_i)$ is a window function of duration Δt of the Gaussian form,

$$w(t - t_i) = \frac{1}{\sqrt{2\pi}\Delta t} \exp\left(-\frac{(t - t_i)^2}{2\Delta t^2}\right). \tag{3}$$

The above formulation actually means that the window function is slided along the time-series and the number of spikes is counted within the window at each location. What is crucial for the present purpose is the window duration Δt. For relatively small Δt, the amplitude of the firing rate corresponds to the spiking activity. Thus, bursts, which are actually regions of high spiking activity, correspond to firing rate spikes whereas silent regions correspond to minima or zeros of the firing rate.

An example of the above formulation for an assembly consisting of two iron electrodes at distance $d = 3$ mm is shown in Fig. 2. The distance between working and reference is $l = 5$ mm and the interaction between the electrodes in excitatory (positive). The electric current, I_1 and I_2, flowing through the two electrodes consists of a silent

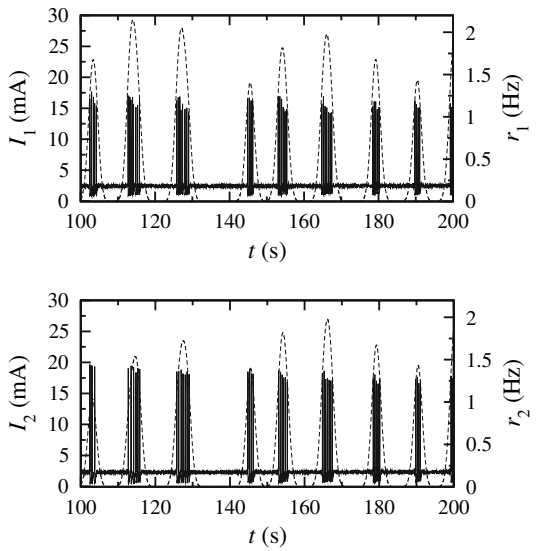

Fig. 2 Electrochemical bursting activity I_i(*full line*) for an assembly of two iron electrodes with distance $d = 3$ mm, together with the corresponding firing rate r_i (*dashed line*) for $\Delta t = 1$ s. Electrode potential $V = 275$ mV, distance between the assembly and reference electrode $l = 5$ mm

state interrupted by regions of fast current spikes (full line). Together with the current time-series, the corresponding firing rates, r_1 and r_2, are plotted, for $\Delta t = 1$ s (dashed line). As can be seen, each oscillation of r_i corresponds to an electric current burst. Moreover, the amplitude of r_i is determined by the number of current spikes within the burst. Apparently, zeros of r_i correspond to silent electric response.

From the experimental result presented in Fig. 2 it is evident that the two coupled electrodes are burst-synchronized, in the sense that electric bursts occur simultaneously. In order to show that burst synchronization actually occurs, the phase of the firing rates is calculated by means of the Hilbert transform [31, 32]. Thus, in order to calculate the instantaneous phase of the firing rate, an analytic signal is constructed, defined as the complex function,

$$\zeta_i(t) = r_i(t) + j\tilde{r}_i(t) = R_i(t)e^{j\phi_i(t)} \tag{4}$$

where $r_i(t)$ is the firing rate of the current flowing through the $i-$th electrode, $R_i(t)$ the instantaneous amplitude of the analytic signal, $\phi_i(t)$ the instantaneous phase and $j = \sqrt{-1}$. The Hilbert transform, $\tilde{r}_i(t)$ of the firing rate $r_i(t)$ is given be the integral,

$$\tilde{r}_i(t) = \frac{1}{\pi} \int_{-\infty}^{+\infty} \frac{r_i(\tau)}{t - \tau} d\tau \tag{5}$$

which can be calculated easily by means of the Fourier transform [32]. It must be noted that in order to calculate the Hilbert transform and the instantaneous phase, the DC

component of the firing rate was removed before the computations.

The instantaneous phases $\phi_1(t)$ and $\phi_2(t)$ together with the phase difference $\Delta\phi(t)$ for the current time-series and the corresponding firing rates presented in Fig. 2 are shown in Fig. 3. As can be seen, the evolution of the phases is almost identical (the two traces are actually overlapped) and the phase difference is almost zero. Therefore, it can be concluded that in this case in-phase burst synchronization is observed.

An additional example of in-phase burst synchronization is presented in Fig. 4 for an electrochemical array consisting of two iron electrodes at distance $d = 8$ mm. In this case, the electrochemical interfaces are weakly coupled due to the distance d. Moreover, the reference electrode is placed very close to the electrode surface, $l = 1$ mm and thus the interaction between the two electrodes is negative (inhibitory). As can be seen, the firing rates r_i correspond to bursting activity and occur simultaneously for both oscillating electrodes.

In-phase burst synchrony is manifested also by plotting the phases of the firing rates together with the phase difference, as shown in Fig. 5. For the first 260 s, the phase difference $\Delta\phi$ is almost zero, i.e. electrochemical bursts are synchronized in-phase. As bursting activity becomes more irregular for $t > 260$ s, electrochemical bursts tend to desynchronize since $\Delta\phi \neq 0$.

Electrochemical burst synchronization occurs for $d = 3$, 5, 8 mm and any value of l, as far as the applied potential is close to the transition from the state of electrodissolution to the oscillatory state, i.e. where elliptic electrochemical bursting oscillations are observed.

The response of an assembly consisting of two oscillatory electrodes is drastically different when V is set at a more anodic value. In this case, electrochemical bursting is classified as square wave and both wave form and period

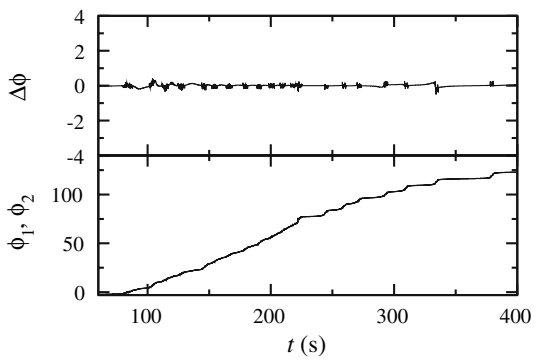

Fig. 3 Firing rate phases, ϕ_1 and ϕ_2, of the current bursts of an assembly of two iron electrodes (traces overlapped), together with the phase difference $\Delta\phi$. Parameter values: $d = 3$ mm, $l = 5$ mm, $V = 275$ mV and $\Delta t = 1$ s

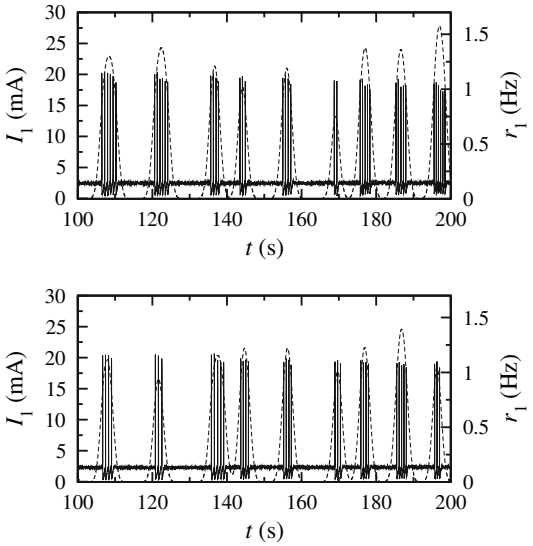

Fig. 4 Electrochemical bursting activity I_i(*full line*) for an assembly of two iron electrodes with distance $d = 8$ mm, together with the corresponding firing rate r_i (*dashed line*) for $\Delta t = 1$ s. Electrode potential $V = 280$ mV, distance between the assembly and reference electrode $l = 1$ mm

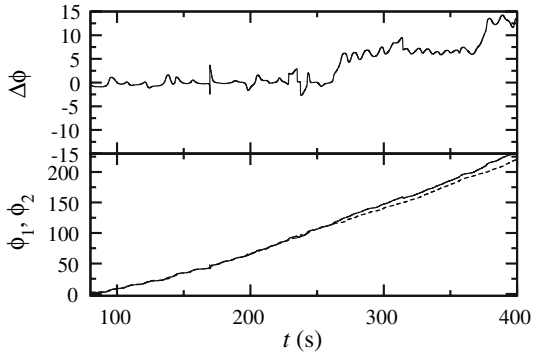

Fig. 5 Firing rate phases, ϕ_1 and ϕ_2, of the current bursts of an assembly of two iron electrodes, together with the phase difference $\Delta\phi$. Parameter values: $d = 8$ mm, $l = 1$ mm, $V = 280$ mV and $\Delta t = 1$ s

are different compared to those in the case of elliptic electrochemical bursting observed for more cathodic potentials. In this case, the slow dynamics can be extracted from the electric current time series by using a low pass filter [33].

A typical example of two interacting iron electrodes for $V = 420$ mV is presented in Fig. 6a. In this case, the distance between the electrodes is $d = 3$ mm and the distance between the reference and working electrodes is $l = 1$ mm. Due to the value of d and l, the interaction is strong and inhibitory (negative). Together with the electric current time-series, the slow dynamics I_s are also shown, extracted from the experimental signals by means of a low pass filter. As can be seen in this figure, in-phase or out-of-phase burst synchronization is not achieved, even though we can

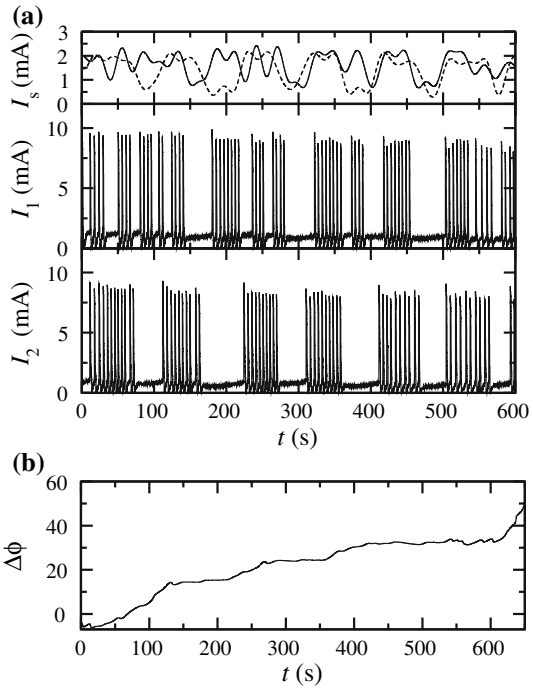

Fig. 6 **a** Electric current time-series, I_1 and I_2, of two coupled iron electrodes for $V = 420$ mV, together with the slow dynamics I_s. **b** Phase difference of the firing rates. Parameter values: $d = 3$ mm, $l = 1$ mm

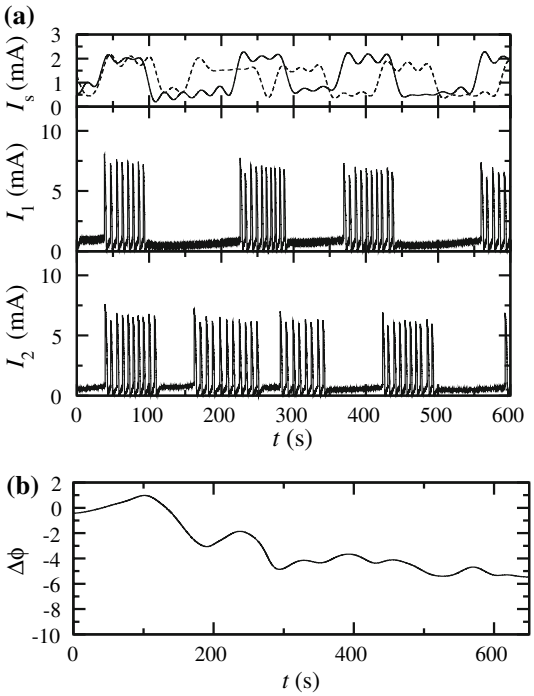

Fig. 7 **a** Electric current time-series, I_1 and I_2, of two coupled iron electrodes for $V = 430$ mV, together with the slow dynamics I_s. **b** Phase difference of the firing rates. Parameter values: $d = 3$ mm, $l = 7$ mm

distinguish some time intervals where the phase difference is constant. The phase-locking intervals can be seen in Fig. 6b where the evolution of the difference of the instantaneous phases of the firing rates is presented.

Lack of in-phase or out-of-phase electrochemical burst synchronization is observed in the case of two iron electrodes interacting in a excitatory manner (positive) when V is close to the transition from the passive to the oscillatory state. As can be seen in the case presented in Fig. 7 for $V = 430$ mV, electrochemical burst synchrony is not observed even though the coupling is strong ($d = 3$ mm) and the interaction is excitatory ($l = 7$ mm).

3.2 Synchronization of electrochemical spikes

Burst synchronization depends strongly on the type of electrochemical bursting but seems to be independent of the type of interaction between the two electrochemical interfaces. No matter if the interaction is excitatory (positive) or inhibitory (negative), electrochemical bursts synchronize in-phase, as far as the bursting is of elliptic type.

On the contrary, synchronization of the fast, spike oscillations (within each burst) depend strongly on the type of interaction. As mentioned previously, small distance l between working-reference electrodes leads to inhibitory interactions whereas large l leads to excitatory interactions. A typical example of spike synchronization for large l is

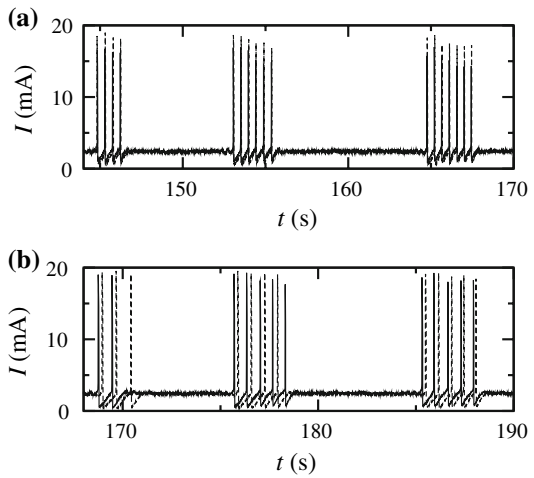

Fig. 8 Synchronization of electric current spikes during electrochemical bursting activity. **a** In-phase spike synchronization for $d = 5$ mm, $l = 3$ mm and $V = 275$ mV and **b** out-of-phase spike synchronization for $d = 8$ mm, $l = 1$ mm and $V = 280$ mV

presented in Fig. 8a. It is evident that fast current spiking occurs almost simultaneously (traces are actually overlapped) and thus in-phase spike synchronization is observed.

For small l the mode of synchronization is different. As can be seen in Fig. 8b current spiking occurs at an almost

constant phase difference. Apparently, the phase is fluctuating but spiking never occurs simultaneously, i.e. current spikes of one electrode always anticipate those of the other electrode. It must be noted that due to experimental imperfections the electrodes are not identical and thus more complex spike synchronization modes can be observed [34]. Even in the case of more complex spike synchronization though, excitatory interactions lead to in-phase spike synchrony and inhibitory interaction to almost out-of-phase synchrony.

A spike synchronization response diagram during elliptic electrochemical bursting is presented in Fig. 9. Thus, for small values of working/reference electrode distance l there is a range of the working/working electrode distance d where the interaction is inhibitory and electric spikes are synchronized out-of-phase (white circles). For larger values of l the interaction is excitatory and electric spikes are in-phase synchronized (black circles). Between these two parameter regions there is a "gray zone" region (triangles) where the response of the interacting electrodes is mixed, i.e. either both in-phase and out-of-phase synchrony is observed within the course of a single experimental trail or the two electrodes behave completely independently.

4 Discussion and conclusions

The electrodissolution/passivation of iron in sulfuric acid, in the presence of small amounts of chloride ions, proceeds via spontaneous currents bursting oscillations within a specific region of applied potential values. During this oscillatory activity the electrochemical interface transits through two different stable states. A silent state where the current attains a constant value and electrodissolution occurs though a porous salt or oxide layer, and an oscillatory state where the electrode surface shifts spontaneously from an almost complete passive state to an electrodissolving state. Moreover, the type of electrochemical bursting activity (elliptic or square wave) depends on the value of the applied potential.

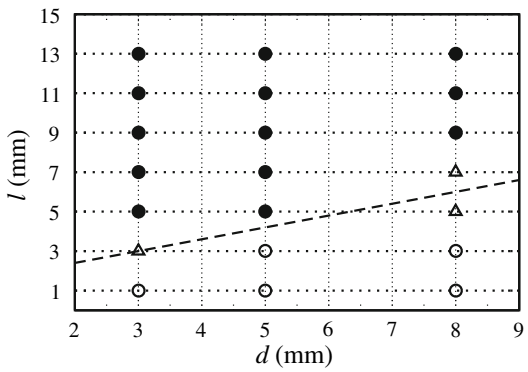

Fig. 9 Spike synchronization response diagram during elliptic electrochemical bursting. *White circles*: inhibitory coupling/out-of-phase spike synchronization. *Black circles*: excitatory coupling/in-phase spike synchronization. *Triangles*: Mixed response

When two iron electrodes interact through the electrolyte, electrochemical bursts are synchronized as far as the bursting is of elliptic type. The synchronization mode does not depend on the type of interaction (excitatory or inhibitory) and thus only in-phase burst synchronization is observed. Additionally, in-phase burst synchronization is very difficult to achieve in the case of square wave electrochemical bursting.

On the other hand, current spike synchronization is determined by the type of interaction. Since the type of interaction in the case of electrochemical systems can be controlled by the position of the reference electrode, both in-phase and out-of-phase spike synchronization in observed experimentally.

The synchronization of electrochemical bursting can be analyzed by calculating the firing rate (elliptic bursting) or by extracting the slow burst dynamics by low-pass filtering (square wave bursting). The above methods in combination with the construction of an analytic signal from the time-series can be used to characterize the type of synchronization.

The synchronization modes of electrochemical networks have been studied in the past for the case of periodic [15, 17, 35] as well as chaotic electrochemical oscillations [36–38]. Coupled bursters have been studied previously in the field of neurophysiology but the present work is the first attempt to elucidate the synchronization properties of coupled electrochemical bursting oscillations. Indeed, the above experimental findings are in very good agreement with similar studies on neural burst synchronization [28, 39, 40]. Similarly to the present electrochemical system, bursting neural cells of elliptic type are synchronized in-phase, no matter if the neural network is coupled through excitatory or inhibitory synaptic connections. On the other hand, square wave neurons are very difficult to synchronize, similarly to the electrochemical analogue. Finally, neural action potential spikes within the bursts tend to synchronize in-phase or out-of-phase for excitatory and inhibitory coupling, respectively, a fact also observed during the electrodissolution/passivation of iron. The similarities between the neurophysiological and electrochemical non-linear dynamic activity can be utilized for the experimental investigation of complex neural behavior by simple electrochemical analogues and even fabricate electrochemical systems to perform simple neural processing functions.

References

1. Heathcote H (1907) J Soc Chem Ind 26:899
2. Lillie R (1920) J Gen Physiol 3:107
3. Lillie R (1925) J Gen Physiol 7:473
4. Lillie R (1936) Biol Rev 11:181
5. Bonhoeffer K (1948) J Gen Physiol 32
6. Bonhoeffer K (1953) Naturwiss 40:301
7. Bonhoeffer K (1955) Angew Chem 67:1
8. Franck U (1956) Prog Biophys Chem 6:171
9. Franck U (1978) Angew Chem 17:1
10. Hudson J, Tsotsis T (1994) Chem Eng Sci 49:1493
11. Koper M (1996) In: Progogine I, Rice S (eds.) Advances in chemical physics, vol XCII. Wiley, New York, pp 161–298
12. Krischer K (2002) In: Alkire R, Kolb D (eds.) Advances in electrochemical science and engineering, vol 8. Wiley-VCH, Verlag, pp 89–208
13. Karantonis A, Miyakita Y, Nakabayashi S (2002) Phys Rev E 65:046213
14. Miyakita Y, Karantonis A, Nakabayashi S (2002) Chem Phys Lett 362:461
15. Karantonis A, Pagitsas M, Miyakita Y, Nakabayashi S (2003) J Phys Chem B 107:14622
16. Karantonis A, Pagitsas M, Miyakita Y, Nakabayashi S (2004) J Phys Chem B 108:5836
17. Miyakita Y, Nakabayashi S, Karantonis A (2005) Phys Rev E 71:056207
18. Karantonis A, Pagitsas M, Yasuyuki Y, Nakabayashi S (2005) Electrochim Acta 50:5056
19. Karantonis A, Pagitsas M, Miyakita Y, Nakabayashi S (2006) Int J Bifurc Chaos 16:1951
20. Karantonis A, Koutsaftis D, Kouloumbi N (2008) Chem Phys Lett 460:182
21. Christoph J, Otterstedt R, Eiswirth M, Jaeger N, Hudson J (1999) J Chem Phys 110:8614
22. Christoph J, Eiswirth M (2002) Chaos 12:215
23. Plenge F, Li YJ, Krischer K (2004) J Phys Chem B 108:14255
24. Sazou D, Pagitsas M, Georgolios C (1992) Electrochim Acta 37:2067
25. Sazou D, Pagitsas M, Georgolios C (1993) Electrochim Acta 38:2321
26. Sazou D, Diamantopoulou A, Pagitsas M (2000) J Electroanal Chem 489:1
27. Koutsaftis D, Karantonis A, Pagitsas M, Kouloumbi N (2007) J Phys Chem C 111:13579
28. Izhikevich EM (2000) Int J Bifurc Chaos 10:2553
29. Dayan P, Abbott L (2001) Theoretical neuroscience: computational and mathematical modeling of neural systems. The MIT Press, Massachusetts
30. Rieke F, Warland D, de Ruyter-van Steveninck R, Bialek W (1999) Spikes: exploring the neural code. MIT press, Massachusetts
31. Rosenblum M, Kurths J (1998) In: Kantz H, Kurths J, Mayer-Kress G (eds.) Nonlinear analysis of physiological data. Springer, Berlin
32. Pikovsky A, Rosenblum M, Kurths J (2001) Synchronization: a universal concept in nonlinear sciences. Cambridge University Press, Cambridge
33. Elson R, Selverston A, Huerta R, Rulkov N, Rabinovich M, Abarbanel H (1998) Phys Rev Lett 81:5692
34. Karantonis A, Koutsaftis D, Kouloumbi N (2009) Electrochim Acta. doi:10.10.16/j.electacta.2009.01.060
35. Kiss I, Wang W, Hudson J (1999) J Phys Chem B 103:11433
36. Wang W, Kiss I, Hudson J (2000) Chaos 10:248
37. Kiss I, Gáspár V, Hudson J (2000) J Phys Chem B 104:7554
38. Kiss I, Wang W, Hudson J (2000) Phys Chem Chem Phys 2:3847
39. Izhikevich E (2000) SIAM J Appl Math 60:503
40. Izhikevich E (2001) SIAM Rev 43:315